

**Two zinc metal-organic framework isomers based on pyrazine
tetracarboxylic acid and dipyridinylbenzene for adsorption and
separation of CO₂ and light hydrocarbons**

Yu Ye^a, Jianfeng Du^a, Libo Sun^b, Yuchuan Liu^a, Shun Wang^a, Xiaowei Song^{a,*},
Zhiqiang Liang^{a,*}

^a*State Key Laboratory of Inorganic Synthesis and Preparative Chemistry, Jilin University, Changchun 130012, P. R. China*

^b*School of Chemical and Biomedical Engineering, Nanyang Technological University, 62 Nanyang Drive 637459, Singapore*

*Corresponding Authors.

E-mail addresses: xiaoweisong@jlu.edu.cn (X. W. Song), liangzq@jlu.edu.cn (Z. Q. Liang).

Materials and Characterizations

All chemicals reagents were obtained from commercial sources without further purification. H₄TCPP was synthesized according to our previous work. FTIR absorption spectra were recorded within the 400–4000 cm⁻¹ region on a Vacuum Bruker 80V FTIR spectrometer. Powder X-ray diffraction (PXRD) patterns were collected on a Rigaku D-Max 2550 diffractometer using Cu-K α radiation ($\lambda = 0.15418$ nm) in a 2θ range of 4–40° with a scan speed of 6° min⁻¹ at room temperature. The element analysis (C, H, and N) were performed with a PerkinElmer 2400 elemental analyzer. Thermogravimetric analyses (TGA) were performed on a TGA Q500 V20.10 Build 36 thermogravimetric analyzer from room temperature to 800 °C in air atmosphere with a heating rate of 10 °C min⁻¹. Before Thermogravimetric analyses (TGA) measurements, the samples were immersed in anhydrous methanol and replaced with fresh one about 15 cycles for 5 days to remove the guest molecules in the channels and then use supercritical CO₂ to remove methanol molecules in the pore, next used the “outgas” function of the surface area analyzer (Micromeritics ASAP 2420) to dried again at 45 °C for 10 h. The N₂ and CO₂ gas adsorption isotherms were performed on a Micromeritics ASAP 2420 and ASAP 2020 plus surface area and porosity analyzer for **1** and **2**, respectively. CO₂, CH₄, C₂H₆, C₃H₈, C₂H₂, C₂H₄ and C₃H₆ gas adsorption measurements at 273 K and 298 K were performed on Micromeritics ASAP 2020 and 3-Flex instruments.

Crystal structure determination

The single crystal X-ray diffraction (SC-XRD) measurement was recorded on a R-ASIX RAPID diffractometer for **1** and **2** with graphite monochromated Mo K α ($\lambda = 0.71073$ Å) radiation at 293 K. Data processing was obtained using the SAINT processing program. The structures were solved through direct method and refined on F^2 by full-matrix least squares with the SHELX-2014 program package. All the non-hydrogen atoms were refined with anisotropic thermal parameters, while hydrogen atoms on the aromatic rings were placed geometrically with isotropic thermal parameters 1.2 times that of the attached

carbon atoms. Detailed refinement information could be checked from the CIF file. The diffused electron densities resulting from these solvent molecules were removed using the SQUEEZE routine of PLATON. A summary of the related crystallographic date and structure refinement parameters for **1** and **2** could be found in table S1 and table S2. The asymmetric unit of **1** and **2** is plotted in figure S1 and figure S2.

CCDC 1920196 (**1**) and CCDC 1920195 (**2**) contain the supplementary crystallographic data for this paper.

These data can be obtained free of charge via www.ccdc.cam.ac.uk/data_request/cif, or by emailing data_request@ccdc.cam.ac.uk, or by contacting The Cambridge Crystallographic Data Centre, 12 Union Road, Cambridge CB2 1EZ, UK; fax: +44 1223 336033.

Table S1. Crystal data and structure optimization data for **1**.

Name	1	
Formula	C _{13.5} HNO ₂ Zn _{0.5}	
Formula weight	241.84	
Temperature	300(2) K	
Wavelength	0.71073 Å	
Crystal system	Orthorhombic	
Space group	<i>pmma</i>	
	<i>a</i> = 11.6989(3) Å	α = 90°.
Unit cell dimensions	<i>b</i> = 15.3730(4) Å	β = 90°.
	<i>c</i> = 18.3406(6) Å	γ = 90°.
Volume	3298.51(16) Å ³	
Z	8	
Density (calculated)	0.974 g/cm ³	
Absorption coefficient	0.769 mm ⁻¹	
F(000)	960	
Crystal size	0.1 × 0.1 × 0.1 mm	
Theta range for data collection	2.221 to 25.355°	
Reflections collected/ unique	18840 / 3297	
<i>R</i> _{int}	0.0354	
Completeness to theta = 25.242°	99.4 %	
Refinement method	Full-matrix least-squares on <i>F</i> ²	
Data / restraints / parameters	3297 / 29 / 210	
Goodness-of-fit on <i>F</i> ²	1.128	
^a <i>R</i> ₁ , <i>wR</i> ₂ [<i>I</i> > 2σ(<i>I</i>)]	<i>R</i> ₁ = 0.0491, <i>wR</i> ₂ = 0.1609	
<i>R</i> ₁ , <i>wR</i> ₂ (all data)	<i>R</i> ₁ = 0.0553, <i>wR</i> ₂ = 0.1687	
Extinction coefficient	n/a	
Largest diff. peak and hole	0.667 and -0.736 e. · Å ⁻³	

^a*R*₁ = $\sum ||F_o| - |F_c|| / \sum |F_o|$. *wR*₂ = $[\sum [w(F_{o2} - F_{c2})_2] / \sum [w(F_{o2})_2]]^{1/2}$

Table S2. Selected bond lengths [\AA] and angles [$^\circ$] for **1**.

Zn(1)-N(2)	2.007(4)	O(1)#3-Zn(1)-O(1)	88.98(18)
Zn(1)-O(1)#1	2.026(2)	O(2)-Zn(2)-O(2)#1	159.59(14)
Zn(1)-O(1)#2	2.026(2)	O(2)-Zn(2)-O(2)#2	87.19(17)
Zn(1)-O(1)#3	2.026(2)	O(2)#1-Zn(2)-O(2)#2	89.21(17)
Zn(1)-O(1)	2.026(2)	O(2)-Zn(2)-O(2)#3	89.21(17)
Zn(2)-O(2)	2.020(2)	O(2)#1-Zn(2)-O(2)#3	87.19(17)
Zn(2)-O(2)#1	2.020(2)	O(2)#2-Zn(2)-O(2)#3	159.59(14)
Zn(2)-O(2)#2	2.020(2)	O(2)-Zn(2)-N(1)	100.21(7)
Zn(2)-O(2)#3	2.020(2)	O(2)#1-Zn(2)-N(1)	100.21(7)
Zn(2)-N(1)	2.033(4)	O(2)#2-Zn(2)-N(1)	100.21(7)
N(2)-Zn(1)-O(1)#1	100.82(7)	O(2)#3-Zn(2)-N(1)	100.21(7)
N(2)-Zn(1)-O(1)#2	100.82(7)	C(1)-O(1)-Zn(1)	128.7(2)
O(1)#1-Zn(1)-O(1)#2	88.98(18)	C(1)-O(2)-Zn(2)	127.9(2)
N(2)-Zn(1)-O(1)#3	100.82(7)		
O(1)#1-Zn(1)-O(1)#3	86.98(18)		
O(1)#2-Zn(1)-O(1)#3	158.36(14)		
N(2)-Zn(1)-O(1)	100.82(7)		
O(1)#1-Zn(1)-O(1)	158.36(14)		
O(1)#2-Zn(1)-O(1)	86.98(18)		

Symmetry transformations used to generate equivalent atoms:

#1 -x+1/2,-y,z #2 -x+1/2,y,z #3 x,-y,z

Table S3. Crystal data and structure optimization data for **2**.

Name	2
Formula	C ₂₄ H ₈ N ₂ O ₄ Zn
Formula weight	453.69
Temperature	205(2) K
Wavelength	0.71073 Å
Crystal system	Monoclinic
Space group	<i>C</i> 2/ <i>c</i> <i>a</i> = 10.056(2) Å α = 90°. <i>b</i> = 21.013(5) Å β = 97.053(7)°. <i>c</i> = 30.488(7) Å γ = 90°.
Volume	6394(3) Å ³
Z	8
Density (calculated)	0.943 g/cm ³
Absorption coefficient	0.790 mm ⁻¹
F(000)	1824
Crystal size	0.1 × 0.1 × 0.1 mm
Theta range for data collection	2.360 to 25.365°
Reflections collected/ unique	15229 / 5714
<i>R</i> _{int}	0.0658
Completeness to theta = 25.242°	98.0 %
Refinement method	Full-matrix least-squares on <i>F</i> ²
Data / restraints / parameters	5714 / 156 / 317
Goodness-of-fit on <i>F</i> ²	1.014
^a <i>R</i> ₁ , <i>wR</i> ₂ [<i>I</i> > 2σ(<i>I</i>)]	<i>R</i> ₁ = 0.0895, <i>wR</i> ₂ = 0.2488
<i>R</i> ₁ , <i>wR</i> ₂ (all data)	<i>R</i> ₁ = 0.1224, <i>wR</i> ₂ = 0.2647
Extinction coefficient	n/a
Largest diff. peak and hole	2.382 and -0.785 e·Å ⁻³

^a*R*₁ = $\sum ||F_o| - |F_c|| / \sum |F_o|$. *wR*₂ = $[\sum [w(F_{o2} - F_{c2})^2] / \sum [w(F_{o2})^2]]^{1/2}$

Table S4. Selected bond lengths [\AA] and angles [$^\circ$] for **2**.

Zn(1)-O(4)	2.025(5)	C(12)#1-O(1)-Zn(1)	132.7(5)
Zn(1)-O(3)	2.031(5)	C(1)-O(2)-Zn(1)	128.6(5)
Zn(1)-O(2)	2.033(5)	C(12)-O(3)-Zn(1)	118.9(5)
Zn(1)-N(3)	2.036(5)	C(1)#1-O(4)-Zn(1)	126.7(5)
Zn(1)-O(1)	2.042(5)	C(20)-N(3)-Zn(1)	123.4(8)
O(4)-Zn(1)-O(3)	87.7(2)	C(24)-N(3)-Zn(1)	122.1(7)
O(4)-Zn(1)-O(2)	159.6(2)	C(21)-N(3)-Zn(1)	122.3(7)
O(3)-Zn(1)-O(2)	91.6(2)	C(25)-N(3)-Zn(1)	120.6(7)
O(4)-Zn(1)-N(3)	100.6(2)		
O(3)-Zn(1)-N(3)	101.5(2)		
O(2)-Zn(1)-N(3)	99.4(2)		
O(4)-Zn(1)-O(1)	86.4(2)		
O(3)-Zn(1)-O(1)	159.8(2)		
O(2)-Zn(1)-O(1)	87.3(2)		
N(3)-Zn(1)-O(1)	98.6(2)		

Symmetry transformations used to generate equivalent atoms:

#1 -x+3/2,-y+1/2,-z+1 #2 -x+1,y,-z+3/2

#3 -x+1,-y+1,-z+1 #4 -x,-y,-z+1

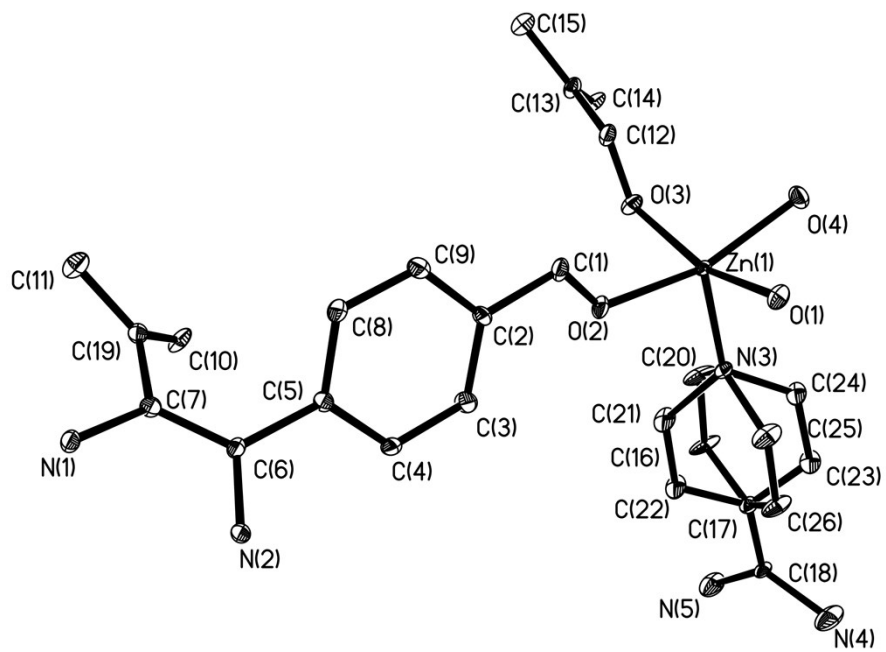


Fig. S1 Representation of the asymmetric unit of **1** showing ellipsoid at the 10% probability level.

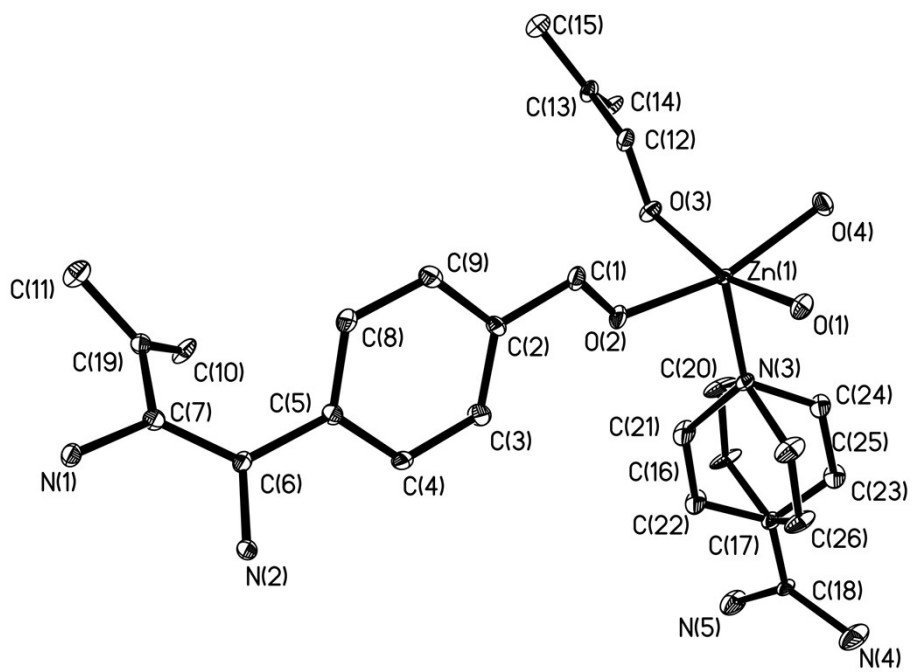


Fig. S2 Representation of the asymmetric unit of **2** showing ellipsoid at the 10% probability level.

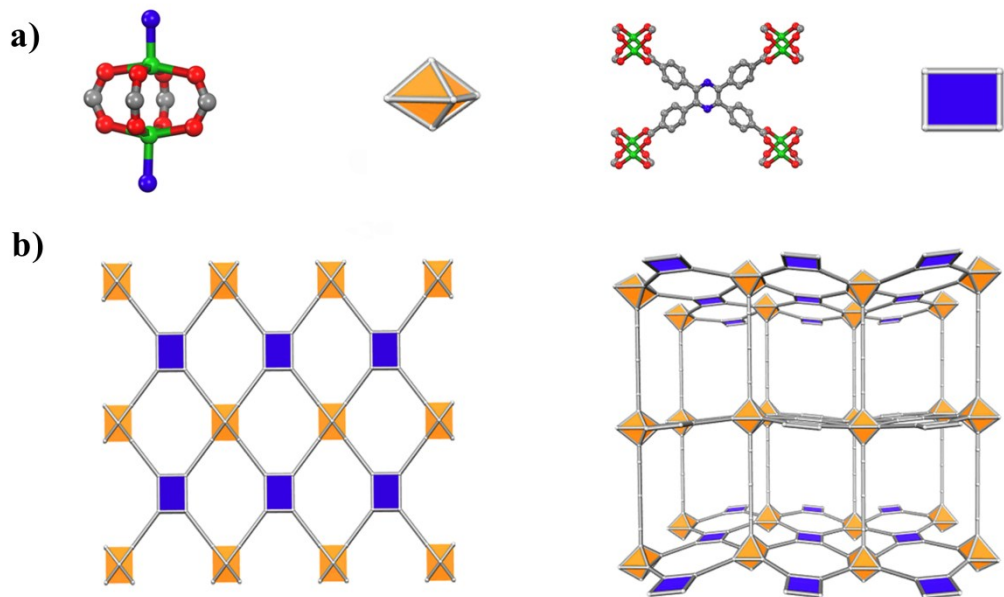


Fig. S3 polyhedral view of the topology of **1**.

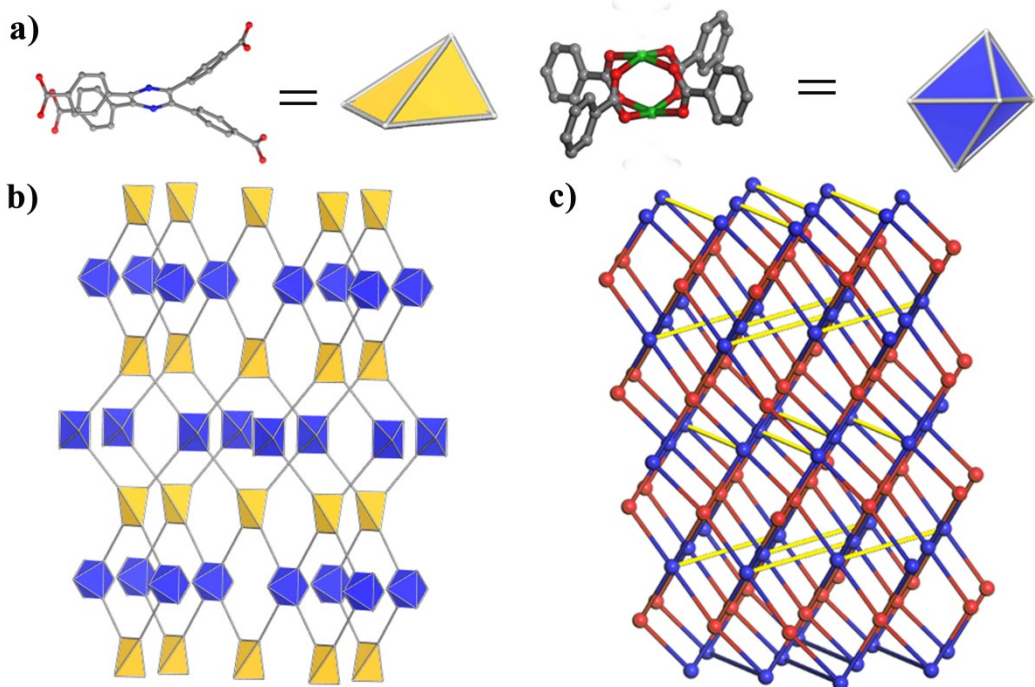


Fig. S4 polyhedral view of the topology of **2**.

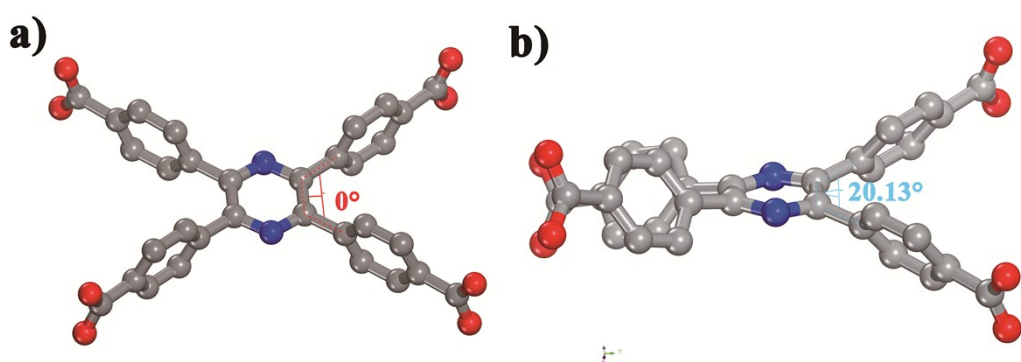


Fig. S5 the dihedral angles of H₄L ligand between benzene ring of **1** and **2**.

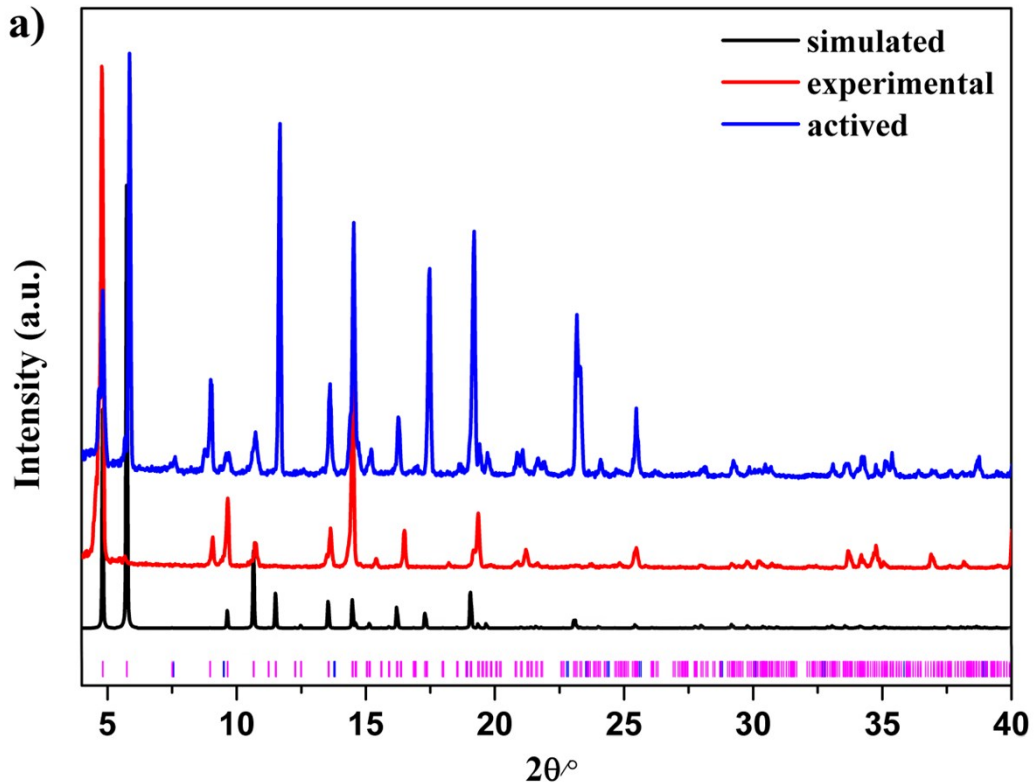


Fig. S6 Powder X-ray diffraction patterns of **1** (as-synthesized, simulated and activated).

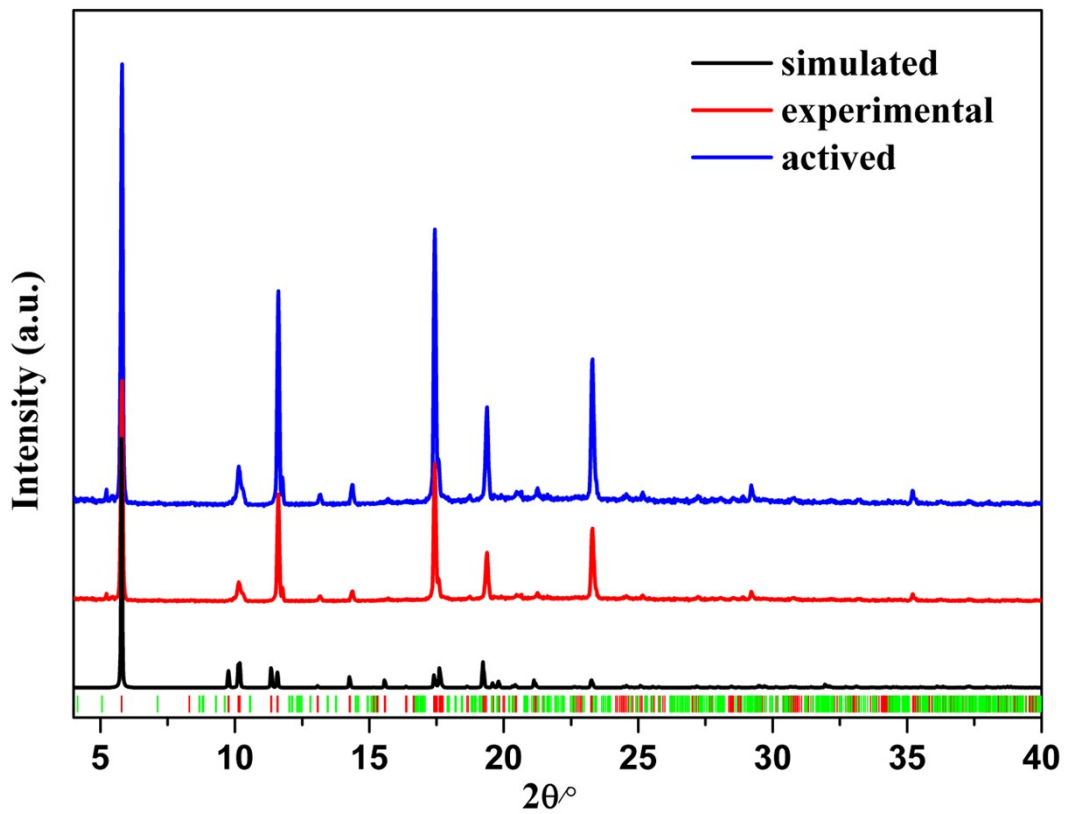


Fig. S7 Powder X-ray diffraction patterns of **2** (as-synthesized, simulated and activated).

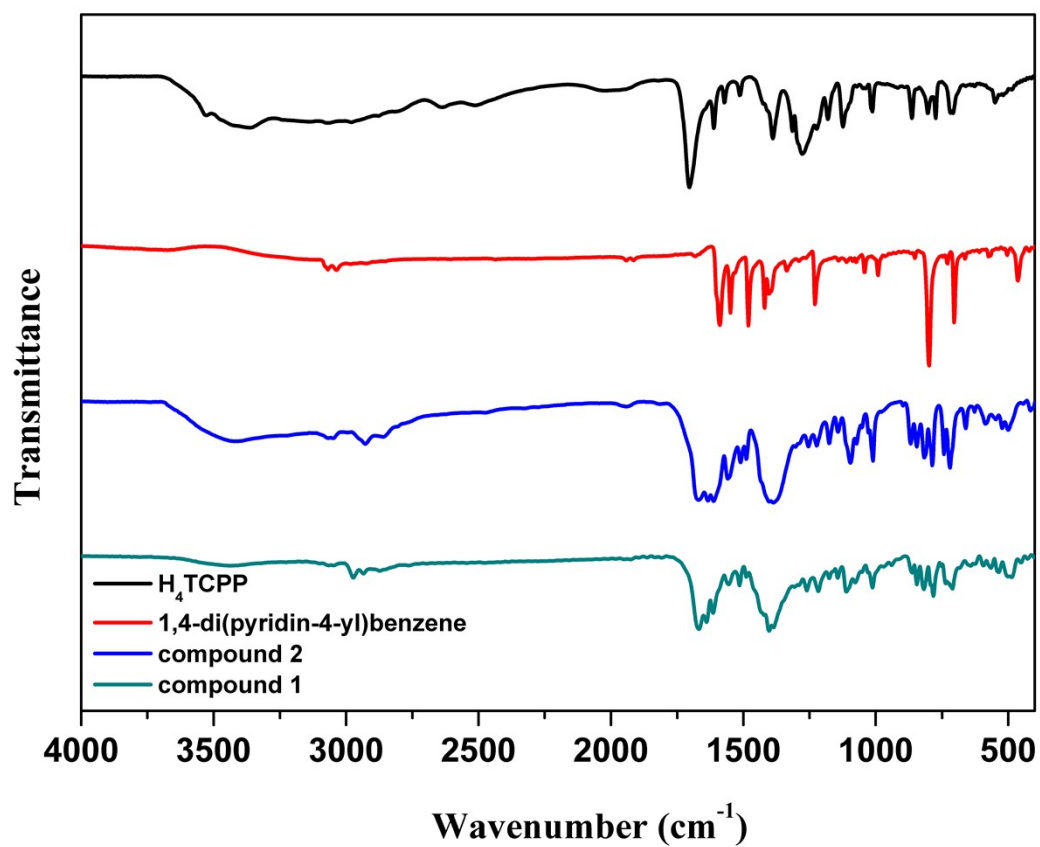


Fig. S8 IR spectra of H₄TCPP, DPB, **1** and **2**.

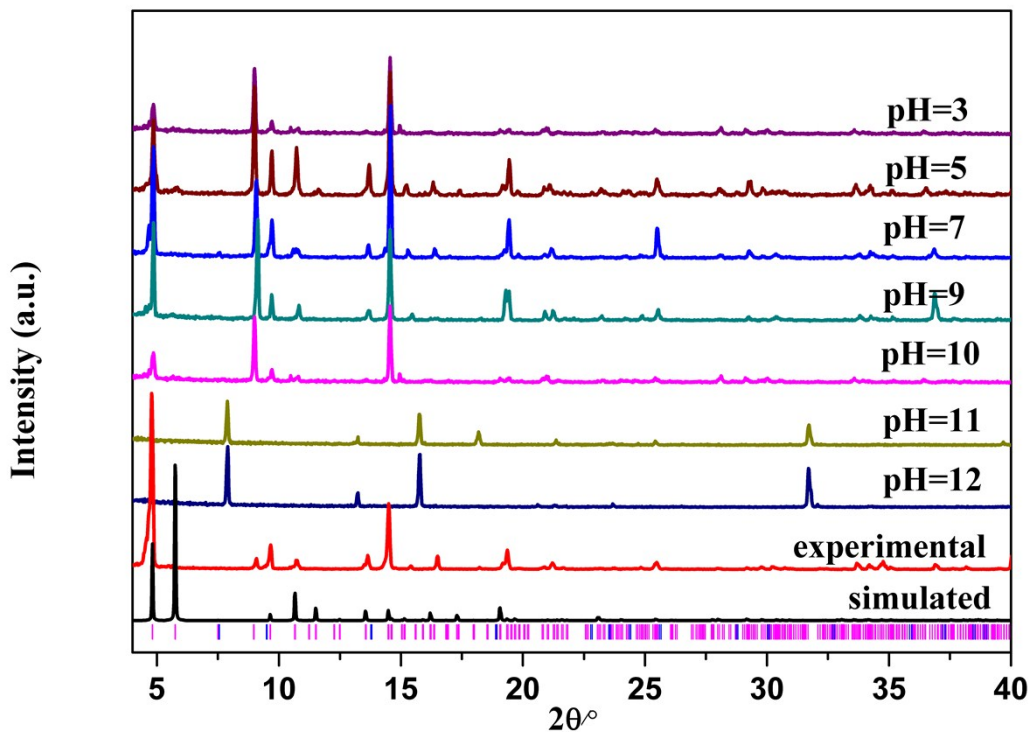


Fig. S9 (a) PXRD patterns of **1** before and after immersed in acidic/alkaline aqueous solutions for 24 h (black: simulated, red: experimental).

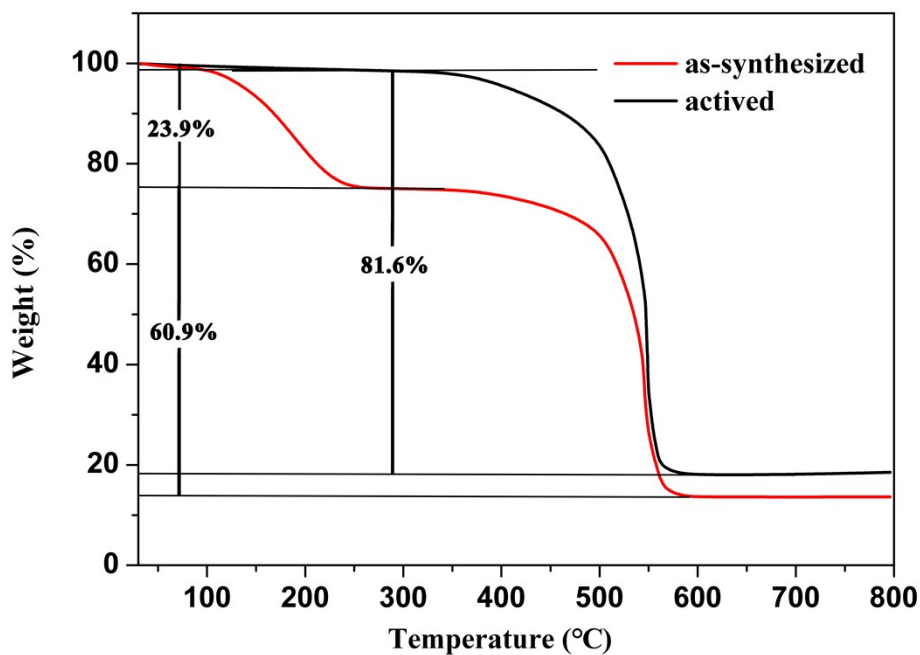


Fig. S10 TGA curves for the as-synthesized and activated **1**.

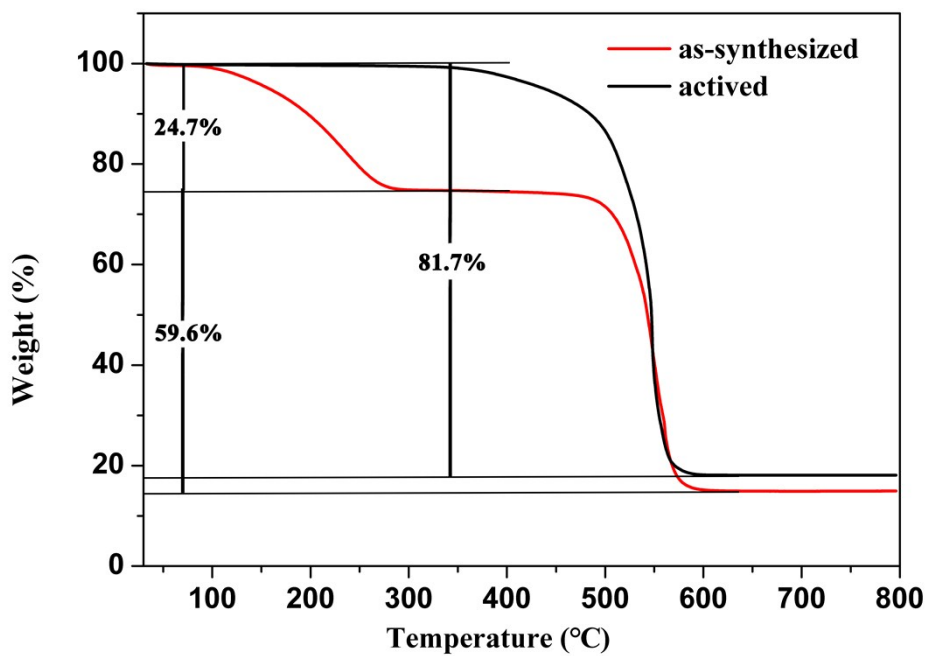


Fig. S11 TGA curves for the as-synthesized and activated **2**.

Heat of Gas Adsorption Calculation

The isosteric heat (Q_{st}) of adsorption for **Zn-TCPP/BPY** was calculated by fitting the CO₂ adsorption isotherms measured at 273 K and 298 K to the virial equation.

$$\ln P = \ln N + \frac{1}{T} \sum_{i=0}^m a_i N^i + \sum_{j=0}^n b_j N^j$$

$$Q_{st} = -R \sum_{i=0}^m a_i N^i$$

N : adsorbed volume (cm³/g);

P : pressure (mmHg);

T : temperature (K);

a_i, b_j : constants;

R : 8.314 J·mol⁻¹·K⁻¹.

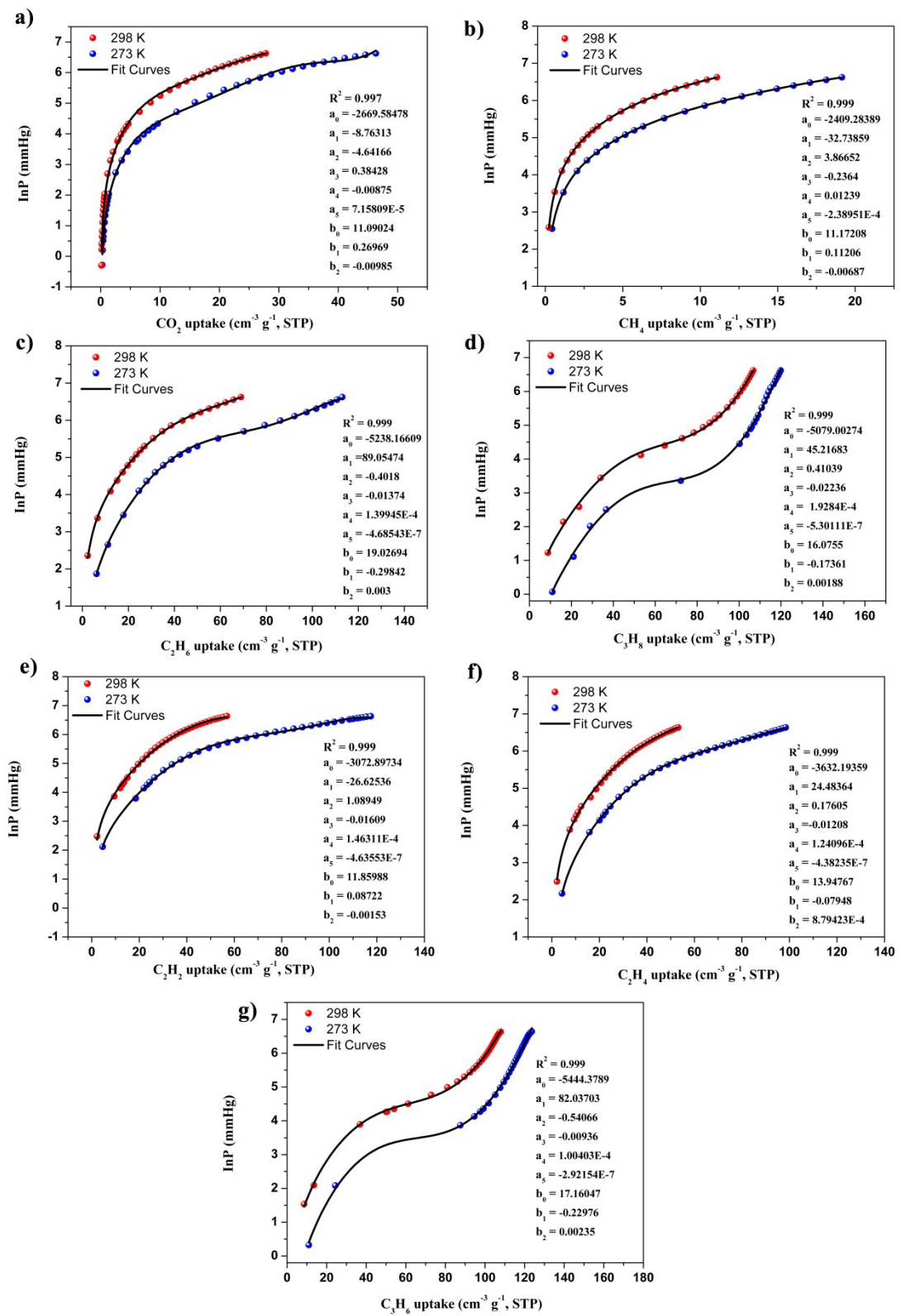


Fig. S12 Virial fitting for CO₂ (a), CH₄(b), C₂H₆(c), C₃H₈(d), C₂H₂(e), C₂H₄(f) and C₃H₆ isotherms of **Compound 1**.

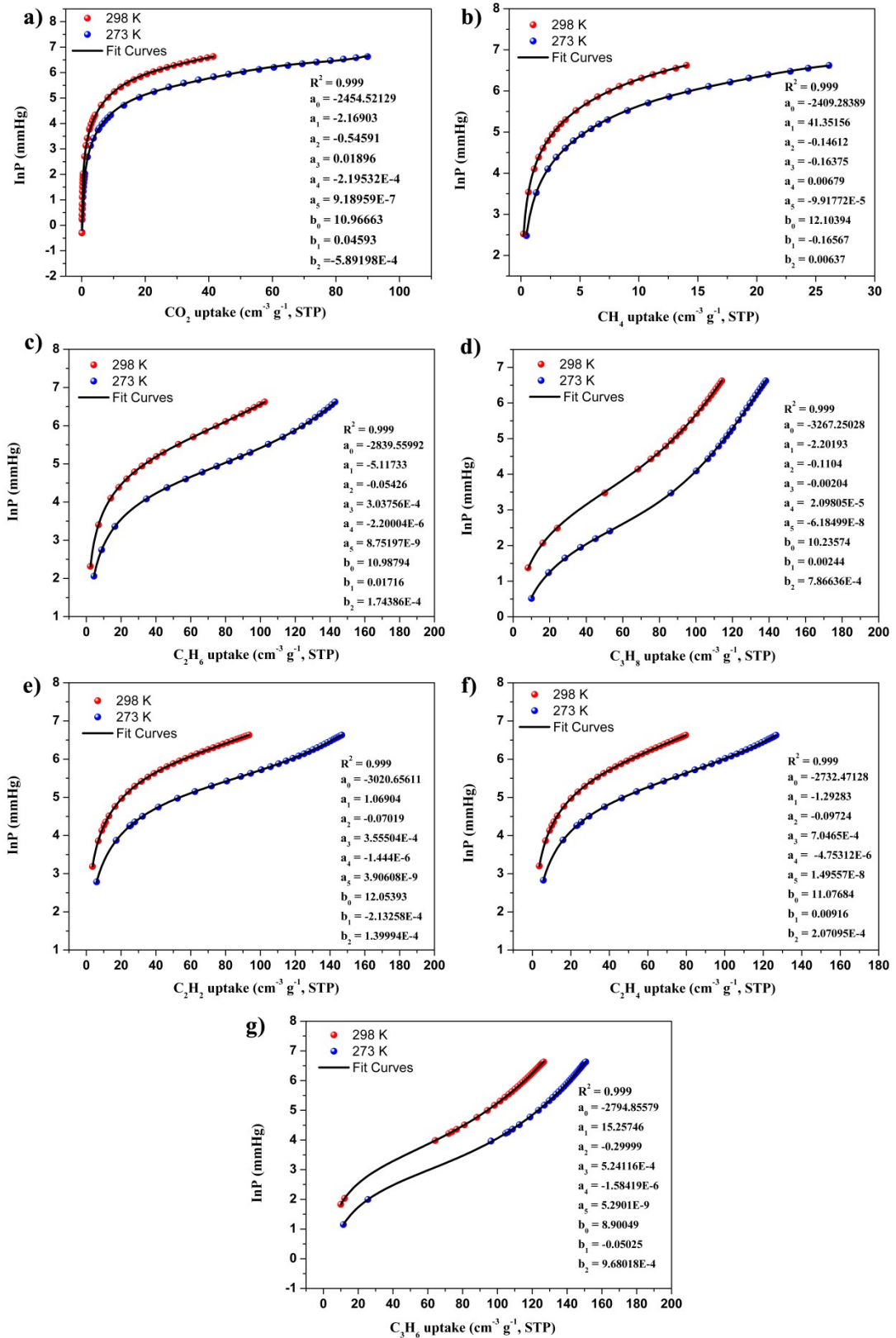


Fig. S13 Virial fitting for CO_2 , CH_4 , C_2H_6 , C_3H_8 , C_2H_2 , C_2H_4 and C_3H_6 isotherms of Compound 2.

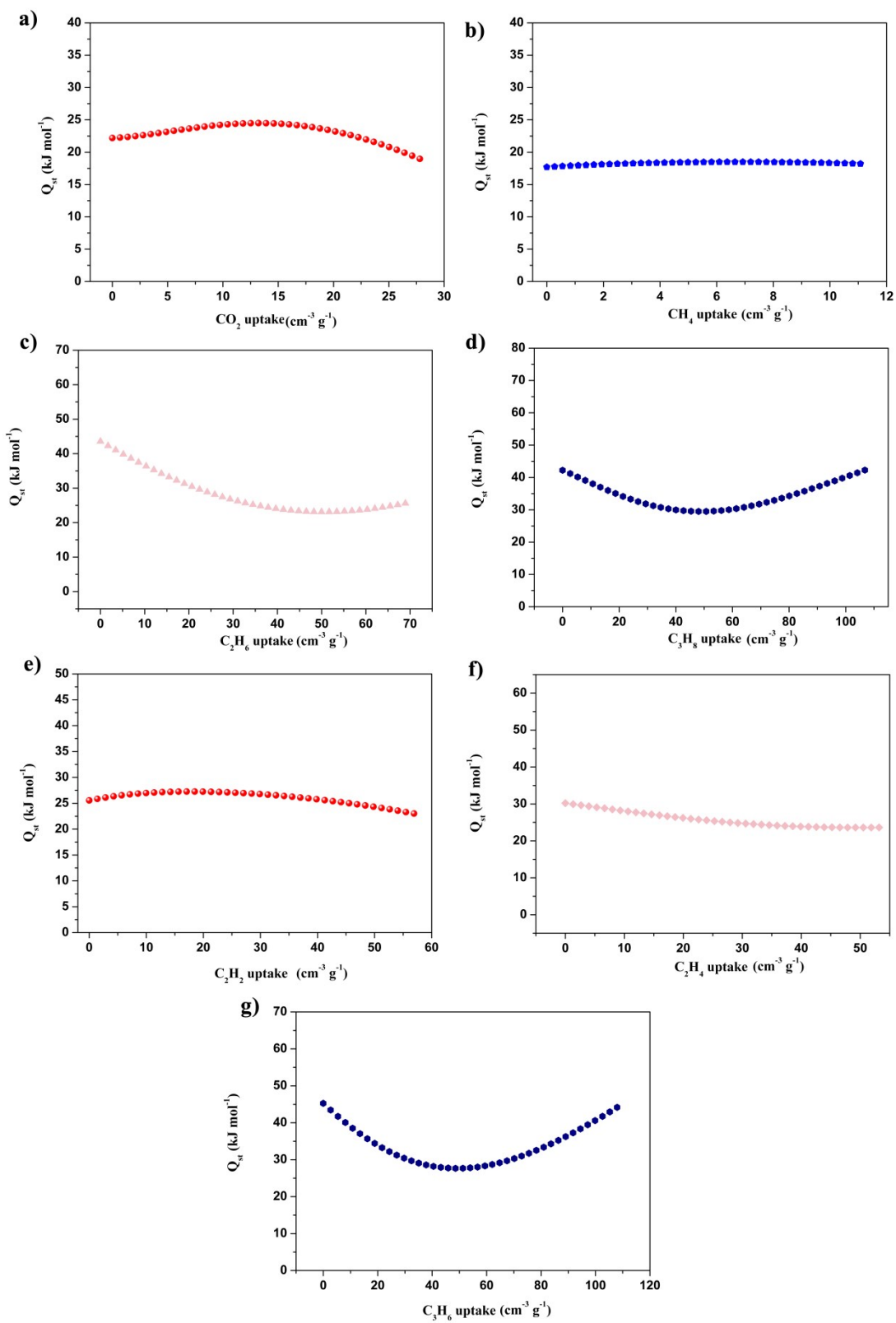


Fig. S14 Isosteric heats of CO_2 , CH_4 , C_2H_6 , C_3H_8 , C_2H_2 , C_2H_4 and C_3H_6 adsorption of Compound 1.

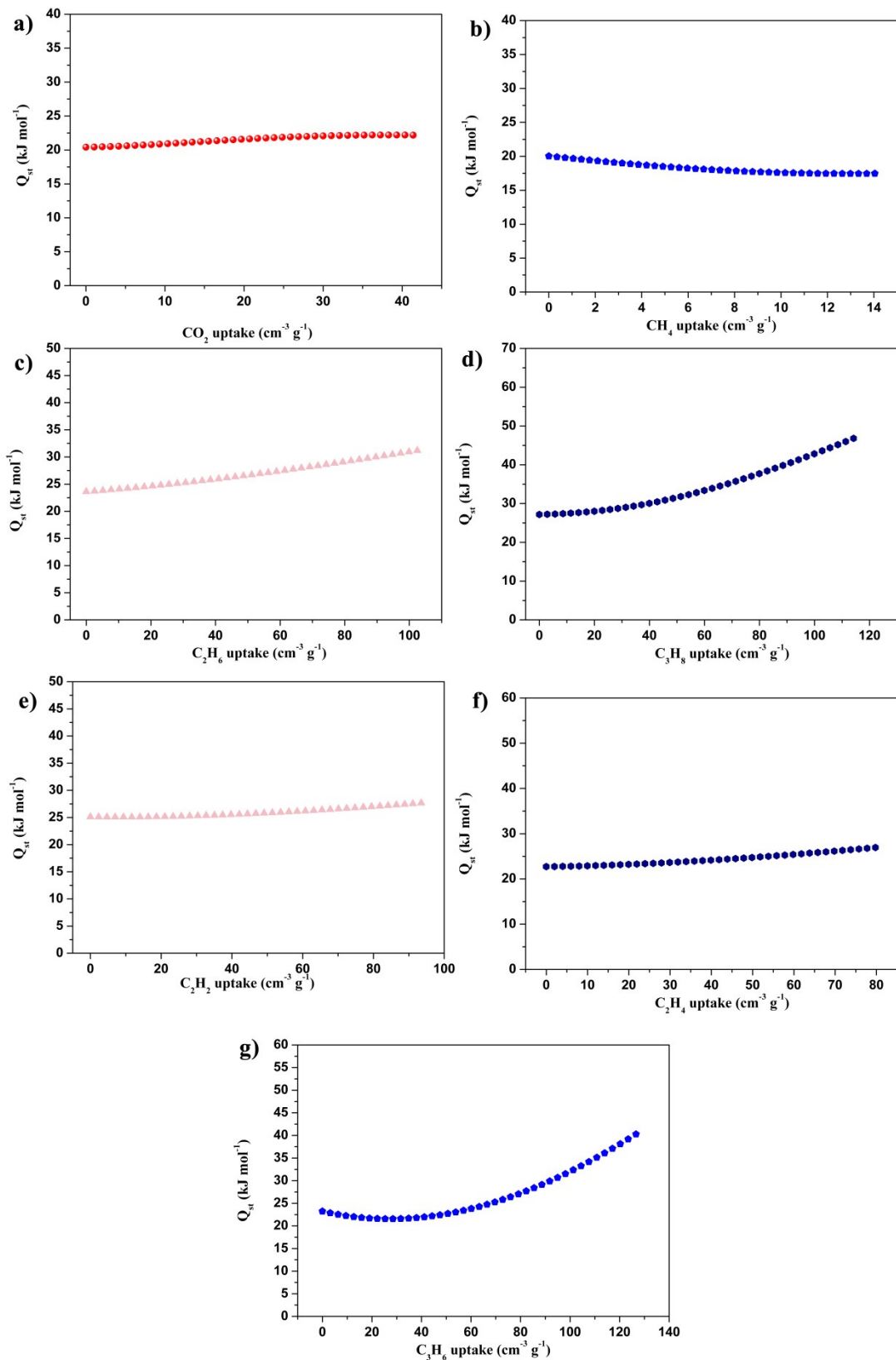


Fig. S15 Isosteric heats of CO_2 , CH_4 , C_2H_6 , C_3H_8 , C_2H_2 , C_2H_4 and C_3H_6 adsorption of **Compound 2**.

Dual-site Langmuir–Freundlich equation

The IAST model is a common method for predicting the adsorption of binary mixed gases by the one-component gas adsorption isotherm obtained by experiments.

$$q = q_{m1} \frac{\frac{1}{b_1 P^{\frac{C_1}{C_1}}}}{1 + b_1 P^{\frac{C_1}{C_1}}} + q_{m2} \frac{\frac{1}{b_2 P^{\frac{C_2}{C_2}}}}{1 + b_2 P^{\frac{C_2}{C_2}}}$$

P: the pressure of the bulk gas at equilibrium with the adsorbed phase (kPa)

q: the adsorbed amount per mass of adsorbent (mol kg^{-1}), q_{m1} and q_{m2} are the saturation capacities of sites 1 and 2 (mol kg^{-1})

b_1 , b_2 : the affinity coefficients of sites 1 and 2 (1/kPa)

C_1 and C_2 are the deviations from an ideal homogeneous surface.

In mixtures containing 1 and 2, perhaps in the presence of other components, preferential adsorption of component 1 over component 2, selectivity can be formally defined as

$$S = \frac{q_1/q_2}{P_1/P_2}$$

q_1 and q_2 : the absolute component loadings (uptake capacities) of the adsorbed phase in the mixture.

Table S5 The refined parameters for the Dual-site Langmuir-Freundlich equations fit for the pure isotherms of CH₄, C₂H₆, C₃H₈, C₂H₂, C₂H₄ and C₃H₆ for **1** at 298 K.

Gas	q_{m1}	b_1	$1/C_1$	q_{m2}	b_2	$1/C_2$	R^2
CH ₄	2.57901	0.00131	0.95469	2.57901	0.00131	0.95469	0.99998
C ₂ H ₆	0.23264	3.4497E-12	6.19054	155.81555	8.80715E-4	0.66404	0.99912
C ₃ H ₈	2.56453	0.1119	1.04818	2.56453	0.1119	1.04824	0.99291
C ₂ H ₂	114.42558	0.00129	0.59889	0.72829	6.9065E-11	4.91634	0.99912
C ₂ H ₄	18.15057	0.00286	0.68993	18.15057	0.00286	0.68993	0.99833
C ₃ H ₆	3.66387	0.17654	0.68183	1.85697	3.9744E-4	3.15212	0.99994

Table S6 The refined parameters for the Dual-site Langmuir-Freundlich equations fit for the pure isotherms of CH₄, C₂H₆, C₃H₈, C₂H₂, C₂H₄ and C₃H₆ for **2** at 298 K.

Gas	q _{m1}	b ₁	1/C ₁	q _{m2}	b ₂	1/C ₂	R ²
CH ₄	0.0201	9.31777E-14	6.64521	57.43506	1.13451E-4	0.99004	0.99998
C ₂ H ₆	5.79869	0.0134	0.99033	1.5754	0.00103	1.85346	0.99999
C ₃ H ₈	2.71751	0.16655	0.92839	2.71751	0.16655	0.92839	0.99788
C ₂ H ₂	6.27864	0.0029	1.11762	6.27864	0.0029	1.11762	0.9998
C ₂ H ₄	4.21581	0.00473	1.09447	4.21581	0.00473	1.09447	0.99992
C ₃ H ₆	3.58385	0.04086	0.72616	3.78537	0.11801	1.33882	0.99999

Table S7. The coordination sequences of **Zn-TCPP** in compound **2**.

N1	1	2	3	4	5	6	7	8	9	10
Num	4	10	24	42	64	90	124	162	204	250
Cum	5	15	39	81	145	235	359	521	725	975
Zn1	1	2	3	4	5	6	7	8	9	10
Num	4	10	24	42	64	92	124	162	204	252
Cum	5	15	39	81	145	237	361	523	727	979

Table S8. The coordination sequences of **Zn-TCPP** in our previous work.^a

N1	1	2	3	4	5	6	7	8	9	10
Num	4	10	24	44	72	104	144	188	240	296
Cum	5	15	39	83	155	259	403	591	831	1127
Zn1	1	2	3	4	5	6	7	8	9	10
Num	4	10	24	44	72	104	144	188	240	296
Cum	5	15	39	83	155	259	403	591	831	1127

^a Y. Y. Jiang, L. B. Sun, J. F. Du, Y. C. Liu, H. Z. Shi, Z. Q. Liang and J. Y. Li, *Cryst. Growth Des.*, 2017, **17**, 2090–2096.

Table S9 Specific data about Porous properties of **1** and **2**

Compound	Total volume(Å ³)	Empty volume(Å ³)	Porosity (%)	Density (g/cm ³)	theoretical pore volumes(cm ³ /g)	experimental pore volumes(cm ³ /g)
1	3298.5	1551.9	47.0	0.974	0.48	0.49
2	6393.6	3151.1	49.3	0.951	0.52	0.50

Table S10 A comparison between compounds **1** for the separation of C₃/CH₄

MOF	C ₃ /CH ₄	selectivity	Ref.
1	C ₃ H ₈ /CH ₄ (0.5/0.5)	122	This work
In/TbCBDA		105	1
LIFM-26		50	2
JLU-MOF51		220	3
[Zn ₂₄ (BDPO) ₁₂ (DMF) ₁₂] · 6DMF · 52H ₂ O		125	4
[(CH ₃) ₂ NH ₂] [Zn ₂ (ABTC)(Tz)] · 3DMF		75	5
[Cu ₄ (PMTD) ₂ (H ₂ O) ₃] · 20H ₂ O		122	6
1		107	This work
UPC-21	C ₃ H ₆ /CH ₄ (0.5/0.5)	75	7
UTSA-35a		90	8
MFM-202a		70	9
tbo-MOF-2		75	10
tbo-MOF-3		178	10

1. D. M. Wang, Z. H. Liu, L. L. Xu, C. X. Li, D. Zhao, G. W. Ge, Z.L. Wang and J. Lin, *Dalton Trans.*, 2019, **48**, 278–284.
2. C. X. Chen, S. P. Zheng, Z. W. Wei, C. C. Cao, H. P. Wang, D. Wang, J. J. Jiang, D. Fenske and C. Y. Su, *Chem.-Eur. J.*, 2017, **23**, 4060–4064.
3. D. M. Wang, J. Zhang, G. H. Li, J. Q. Yuan, J. T. Li, Q. S. Huo and Y. L. Liu, *ACS Appl. Mater. Interfaces*, 2018, **10**, 31233–31239.
4. H. M. He, D.-Y. Zhang, F. Guo, F. X. Sun, *Inorg. Chem.*, 2018, **57**, 7314–7320.
5. L. F. Zou, J. Q. Yuan, Y. Yuan, J. M. Gu, G. H. Li, L. R. Zhang and Y. L. Liu, *CrystEngComm.*, 2019, **21**, 3289–3294.
6. L. K. Meng, Z. Y. Niu, C. Liang, X. L. Dong, K. Liu, G.H. Li, C. G. Li, Y. Han, Z. Shi and S. H. Feng, *Chem. Eur. J.*, 2018, **24**, 13181–13187.
7. M. H. Zhang, X. L. Xin, Z. Y. Xiao, R. M. Wang, L. L. Zhang and D. F. Sun, *J. Mater. Chem. A.*, 2017, **5**, 1168–1175.
8. Y. B. He, Z. J. Zhang, S. C, Xiang, F. R. Fronczek, R. Krishna and B. L. Chen, *Chem. Commun.*, 2012, **48**, 6493–6495.
9. S. Gao, C. G. Morris, Z. Z. Lu, Y. Yan, H. G. W. Godfrey, C. Murray, C. C. Tang, K. M. Thomas, S. H. Yang and M. Schröder, *Chem. Mater.*, 2016, **28**, 2331–2340.

10. Y. Belmabkhout, H. Mouttaki, J. F. Eubank, V. Guillerm and M. Eddaoudi, *RSC Adv.*, 2014, **4**, 63855–63859.